Review article

Costas M. Soukoulis*, Thomas Koschny, Philippe Tassin, Nian-Hai Shen and Babak Dastmalchi

What is a good conductor for metamaterials or plasmonics

Abstract: We review conducting materials like metals, conducting oxides and graphene for nanophotonic applications. We emphasize that metamaterials and plasmonic systems benefit from different conducting materials. Resonant metamaterials need conductors with small resistivity, since dissipative loss in resonant metamaterials is proportional to the real part of the resistivity of the conducting medium it contains. For plasmonic systems, one must determine the propagation length at a desired level of confinement to estimate the dissipative loss.

Keywords: optics; metamaterials; plasmonics; conductors.

DOI 10.1515/nanoph-2014-0013
Received June 4, 2014; accepted September 4, 2014

1 Introduction

Artificial nanophotonic media – photonic crystals (PCs), negative index materials (NIMs), metamaterials (MMs), and plasmonic structures – enable the realization of novel electromagnetic properties unattainable in naturally occurring materials. There has been a truly amazing amount of innovation during the last few years [1–5] and more is yet to come. Spurred by new opportunities, scientists have produced exotic concepts that exploit these new materials: (i) we can now specify how to make a lens whose resolution is limited not by the wavelength of light, but only by our ability to build a material to the necessary specifications [6]; (ii) we can guide radiation along an arbitrary trajectory, for instance to hide an object from sight [7, 8]; and (iii) we can design and manufacture materials with magnetic response in the terahertz and optical domains. Clearly, nanophotonics can develop mold-breaking technologies for a plethora of applications, where control over light (or more generally electromagnetic radiation) is a prominent ingredient – among them telecommunications, solar energy harvesting, biological and terahertz imaging and sensing, optical isolators, nano-lasers, quantum emitters, sensors, polarizers, and medical diagnostics, to name just a few.

However, many serious obstacles must be overcome before the impressive possibilities of MMs and plasmonics, especially in the optical regime, will lead to applications. One of these obstacles is dissipative loss, which needs to be overcome to advance nanophotonic structures towards real-life applications. At this point, we already want to emphasize that a good conducting material for plasmonics is not necessarily the same as a good material for metamaterials. For resonant metamaterials, we need conductors with small resistivity, whereas for plasmonics we need to have large propagation length and high confinement for the surface plasmon polaritons [9, 10].

2 Resonant metamaterials with low loss

Metamaterials are tailored, man-made materials composed of subwavelength building blocks (“photonic atoms”), densely packed into an effective medium [1–4].

***Corresponding author: Costas M. Soukoulis,** Ames Laboratory–US DOE and Department of Physics and Astronomy, Iowa State University, Ames, Iowa 50011, USA; and Institute of Electronic Structure and Lasers (IESL), FORTH, 71110 Heraklion, Crete, Greece, e-mail: soukoulis@ameslab.gov
Thomas Koschny and Nian-Hai Shen: Ames Laboratory–US DOE and Department of Physics and Astronomy, Iowa State University, Ames, Iowa 50011, USA
Philippe Tassin: Department of Applied Physics, Chalmers University, SE-412 96 Göteborg, Sweden
Babak Dastmalchi: Ames Laboratory–US DOE and Department of Physics and Astronomy, Iowa State University, Ames, Iowa 50011, USA; and Institute of Electronic Structure and Lasers (IESL), FORTH, 71110 Heraklion, Crete, Greece

Edited by Volker Sorger

In this fashion, optical properties that simply do not exist in either naturally occurring or conventional artificial materials become reality. A particularly important example of such a photonic atom is the split-ring resonator (SRR) [11] – essentially a tiny electromagnet – which allows for artificial magnetism at elevated frequencies, enabling the formerly missing control of the magnetic component of electromagnetic light waves. Negative magnetic response (i.e., $\mu<0$) above the SRR eigenfrequency, combined with the more usual negative electric response from metal wires (i.e., $\varepsilon<0$), can lead to a negative index of refraction. Following the original theoretical proposal in 1999 [11], MMs were realized at microwave frequencies in 2000 [12] and entered the optical domain (from infrared to the visible) during 2004–2011 [4, 13]. In 2007, negative-index MMs reached the red end of the visible spectrum [4, 14] (see Figure 1 in ref. [4]) and, in 2011, a NIM operating at a free-space wavelength of 660 nm was realized [15].

The field of metamaterials (MMs) has seen spectacular experimental progress in recent years [1–4]. However, large intrinsic losses in metal-based structures have become the major obstacle towards real-world applications, especially at optical wavelengths. Most MMs to date are made with metallic constituents, resulting in significant dissipative loss. These losses originate in the Joule heating caused by the large electric currents in meta-atoms and the poor conductivity of metals and other available conductors at optical frequencies. One promising way of overcoming dissipative loss is based on introducing gain materials in metamaterials [16]. Therefore, it is of vital importance to understand the mechanism of the coupling between a meta-atom and the gain medium [17, 18]. Counter-intuitively, pump-probe experiments of split-ring resonators on top of a gain substrate have revealed that the transmission of a metamaterial may be reduced when gain is added to a metamaterial [19]. Computer simulations have confirmed this effect and attributed it to the characteristic impedance mismatch created by the meta-atom-gain coupling [17]. In addition, these ideas can be used to incorporate gain to obtain new nanoplasmonic lasers [16, 20].

Whether or not a gain medium is added to a metamaterial structure, we want to have strong electric and magnetic resonances to achieve low dissipative loss. We have recently addressed the question of what makes a good conductor for MMs and we have developed a fairly general model of MMs with a single resonance in the magnetic dipole response [9]. It turns out that the fraction of power dissipated in the material can be expressed through a dimensionless figure-of-merit called the dissipation factor, ζ, which is proportional to the real part of the resistivity $\mathrm{Re}(\rho)$. This analysis is valid for all metamaterials with a resonant subwavelength constituent.

Since the figure-of-merit for conductors in resonant MMs comes down to the real part of the (high-frequency) resistivity, we need to identify new materials with smaller resistivity. Finding materials with smaller resistivity would have an important impact on the field of metamaterials [9]. It must be noted here that the imaginary part of the permittivity of different conductors (metals, conducting oxides) may not correctly characterize the corresponding intrinsic losses, but we should adopt the real part of resistivity [$\mathrm{Re}(\rho)$] for the dissipative loss evaluation [9].

In the scope of materials whose response can be satisfactorily described by a Drude model, $\mathrm{Re}(\rho)$ is essentially determined by γ/ω_p^2, where γ is the collision frequency and $\omega_p=2\pi f_p$ represents the plasma frequency. This establishes a good figure-of-merit for conducting materials (noble metals (Ag, Au, Cu), Al, alkali-noble intermetallic alloys (KAu, LiAg), and nitrides of transient metals (ZrN, TiN)) in resonant MMs. For instance, from the fitted Drude model for AZO within 100–300 THz (see Table 1), the characteristic loss term γ/f_p^2 equals 1×10^{-3} [THz^{-1}], while in contrast, for gold within almost the same frequency range (up to 460 THz), the loss term has a much smaller value, 2.45×10^{-5} THz^{-1}. Figure 1 shows the real (left column) and the imaginary (right column) part of permittivity of the conducting oxide AZO (data reproduced from Refs. [21, 24, 25]) and the Drude model fittings [21, 24]. Our Drude fit presented in Table 1, with $\varepsilon_\infty=3.48$, $f_p=366.2$ THz and $\gamma=135.1$ THz, is shown together with the models listed in Refs. [21] and [24] with and without a 2π factor taken into account for the corresponding collision frequency γ. It is

Table 1 Fitted parameters of Drude model and value of γ/f_p^2 (characterizing the ohmic loss) for different materials, i.e., AZO, Au, ZrN and Cu.

Material	Frequency band [THz]	Fitted parameters of Drude model			γ/f_p^2 [THz^{-1}]
		ε_∞	f_p [THz]	γ [THz]	
AZO	100–300	3.48	366.19	135.12	1.00×10^{-3}
Au	150–460	10.67	2186.55	117.33	2.45×10^{-5}
ZrN	200–600	6.65	1988.87	689.77	1.74×10^{-4}
Cu	<40	1	1914	52.40	1.43×10^{-5}

These Drude models are fitted in the indicated frequency band on data from Ref. [21] for AZO and ZrN, data from Ref. [22] for Au, and data from Ref. [23] for Cu. All experimental data is measured on thin films, except for Cu (but Cu is generally only preferred for low-frequency metamaterials where bulk properties are valid).

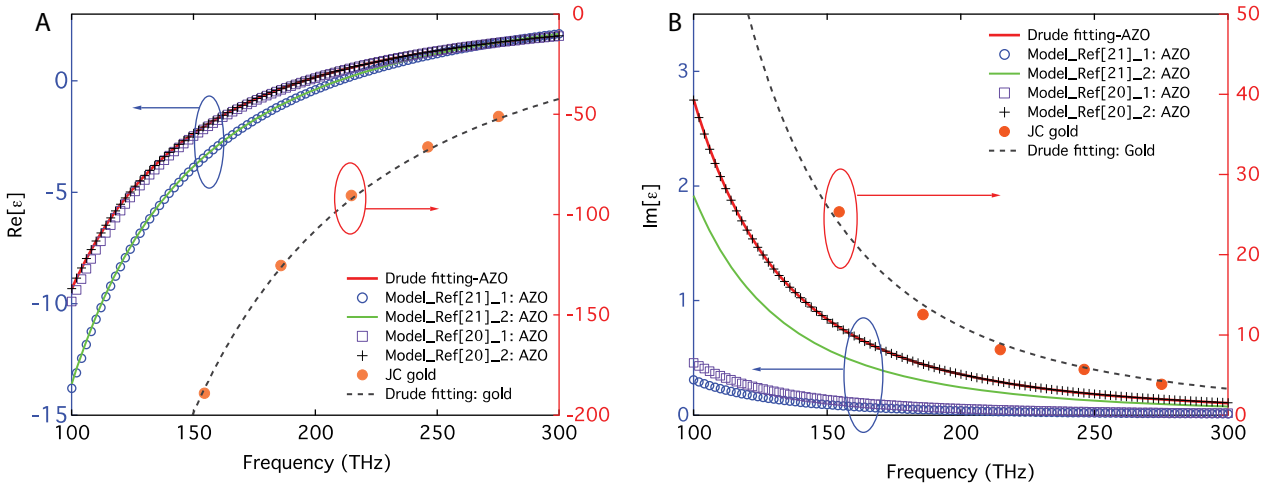

Figure 1 Comparison of data for gold and AZO between 100 and 300 THz: (A) Re(ε) and (B) Im(ε). For AZO, our fitted Drude model is listed together with the models in Refs. [21] and [24] w/ and w/o a 2π factor taken into account in the corresponding collision frequency. For gold, our Drude fitted model is shown consistent with experimental data by Johnson and Christy [22].

found from Figure 1 that, by missing the 2π factor for γ, the Drude model renders an unrealistically low imaginary part of permittivity values (see curves with blue squares and circles). In addition, the experimental Johnson and Christy data [22] for gold are also presented in Figure 1 with our fitted Drude model, for an intuitive comparison to AZO data. However, the imaginary part of permittivity Im(ε) is not a correct figure-of-merit for characterizing conducting materials.

Finally, we illustrate our comparison of conducting materials with the fishnet structure, a typical resonant metamaterial at optical wavelengths. In Figure 2, we show the retrieved effective material parameters – i.e., real part of the refractive index [Re(n)], the permittivity [Re(ε)], and the permeability [Re(μ)] – for an AZO- and a Au-based fishnet metamaterial. The geometry of the fishnet is schematically presented in the inset of Figure 2 (the parameters are given in the figure caption). According to

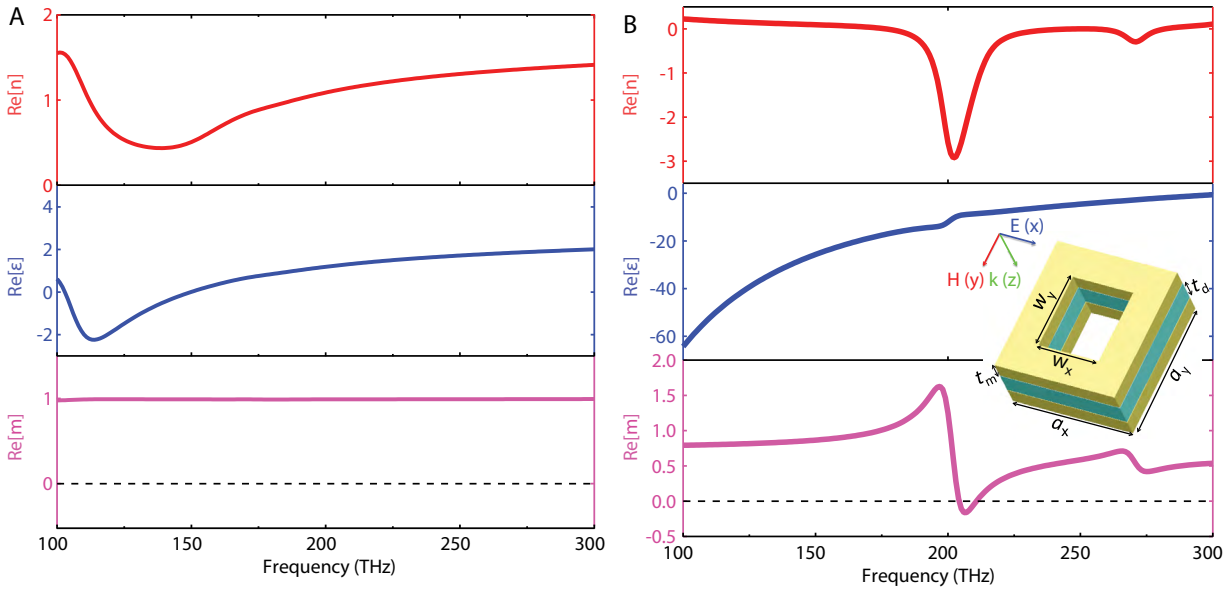

Figure 2 Retrieved real part of effective refractive index [Re(n)], permittivity [Re(ε)], and permeability [Re(μ)] for fishnet structure made by AZO-MgO-AZO (A) and Au-MgO-Au (B), respectively. The fishnet structure [schematically shown as inset of Figure 2(B)] has dimensions a_x=500 nm, a_y=600 nm, w_x=200 nm, w_y=350 nm, t_m=30 nm, and t_d=40 nm.

Figure 2, we find that the fishnet made from Au-MgO-Au possesses a negative index with simultaneously negative ε and μ within some frequency band, but that the AZO-based fishnet does not show any interesting feature of magnetic resonance. This is due to the fairly high intrinsic loss of AZO (see last column of Table 1), dampening the fishnet resonance enough to preclude negative permeability. Based on the data for ZrN within the 200–600 THz frequency band, the loss characterization term γ/f_p^2 equals 1.74×10^{-4}, which is about an order of magnitude larger than that of gold, making the achievement of negative n or μ far from feasible.

3 Surface plasmons with large propagation length

Dissipative loss in plasmonic systems is manifested by the decay of surface plasmon polariton (SPP) excitations (see Figure 3). Unfortunately, there is no simple criterion to estimate the propagation length from a single constitutive parameter. Only if Im(ε)<<|Re(ε)|, a simplified expression can be found, but for many conducting materials, it is not applicable. In addition, there is an intrinsic trade-off between the degree of confinement and the propagation length of a SPP that must be considered. In most cases, therefore, it is necessary to calculate the propagation length from the dispersion relation for a given level of confinement.

Figure 4 provides an overview of the propagation and confinement figures of merit for SPPs at a single material/air interface [10, 26]. The propagation length of an SPP, propagating at the interface in the z-direction (~exp[$i(\beta z-\omega t)$]), can be obtained from $L_p=1/|\mathrm{Im}(\beta)|$. The SPP wavelength is $\lambda_{SPP}=2\pi/|\mathrm{Re}(\beta)|$, and the lateral decay length is $\delta=1/\mathrm{Re}[\sqrt{\beta^2-(\omega/c)^2}]$. We can then define the two figure-of-merits for a plasmonic system: for the propagation length we have $\mathrm{FOM}_{\mathrm{Prop}}=L_p/\lambda_{SPP}$, and for the degree of confinement we have $\mathrm{FOM}_{\mathrm{Conf}}=\lambda_{SPP}/\delta$. Three different degrees of confinement ($\mathrm{FOM}_{\mathrm{Conf}}$=2, 4 and 8) are presented for the comparison in Figure 4.

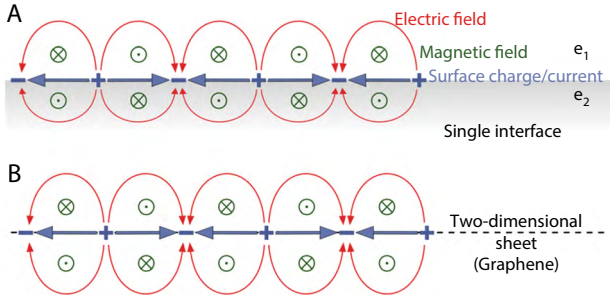

Figure 3 TM surface modes of (A) a single interface structure, (B) a two-dimensional sheet material (e.g., graphene).

At optical frequencies, silver has the longest propagation length of the listed materials (100 SPP wavelengths) at a low degree of confinement ($\mathrm{FOM}_{\mathrm{Conf}}$=2), but at a higher degree of confinement ($\mathrm{FOM}_{\mathrm{Conf}}$=8), it exhibits the shortest propagation length equal to one SPP wavelength. If strong confinement is desired, Al is a better choice for the conducting medium. At around 100 THz, transparent conducting oxides (AZO, ITO GZO) have $\mathrm{FOM}_{\mathrm{Prop}}$=10 for weak confinement and $\mathrm{FOM}_{\mathrm{Prop}}$=2~3 for medium confinement, respectively. At 20–30 THz, SiC with weak confinement ($\mathrm{FOM}_{\mathrm{Conf}}$=2) has a surprisingly large propagation length: its $\mathrm{FOM}_{\mathrm{Prop}}$ is nearly 60. Graphene is another conducting medium that sustains SPP modes [5, 27]. SPPs on graphene are extremely well confined ($\mathrm{FOM}_{\mathrm{Conf}}$=264), but they have rather short propagation lengths ($\mathrm{FOM}_{\mathrm{Prop}}\approx1$) [9]. Recent graphene plasmonics experiments [28] have indeed demonstrated propagation lengths of about one SPP:

$$L_p/\lambda_{SPP}=\frac{1}{2\pi\,\mathrm{Im}(\beta)/\mathrm{Re}(\beta)}=\frac{1}{2\pi\gamma_p}=\frac{1}{2\pi\,0.135}\approx1.18$$

with the plasmon damping rate $\gamma_p\approx0.135$ from Ref. [28]. Nevertheless, graphene remains a fascinating material for terahertz applications [29], because of its atomic thickness, its easy tunability and its extreme subwavelength lateral confinement of surface plasmons. Figure 5 plots the ratio of the surface plasmon wavelength to the free-space wavelength versus frequency in different materials.

4 Conclusions

The lowest dissipative loss in resonant metamaterials on the one hand and plasmonics systems on the other hand is not achieved by the same conductors. For use in resonant metamaterials, the real part of the frequency-dependent resistivity is the correct quantity to judge the merits of the conducting material. For plasmonics applications, the propagation length (dissipative loss) and the degree of confinement of the SPP modes must be determined. We have compared a number of commonly used plasmonic materials while considering the inherent trade-off between propagation length and confinement. We believe it is very worthwhile continuing the research effort to develop better conducting materials, because of the considerable improvement such materials would bring to the nanophotonics field.

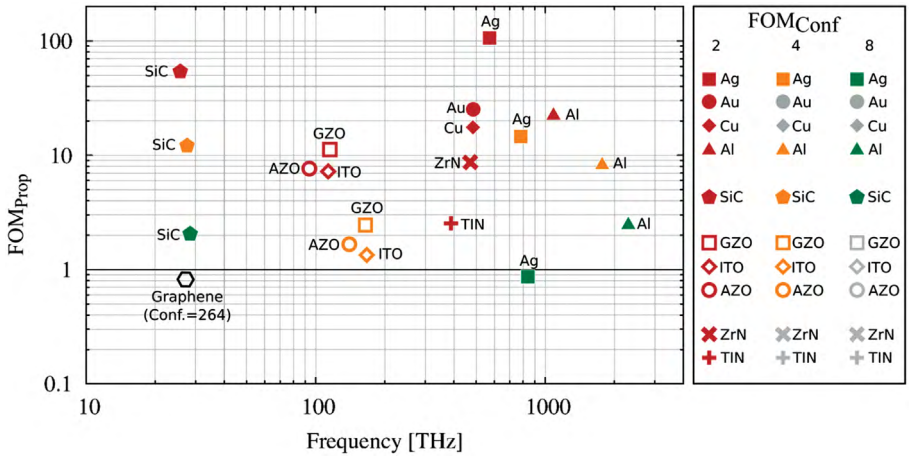

Figure 4 Propagation length of SPPs figure-of-merit (FOM_{Prop}) vs. frequency for different materials at three different FOM_{conf}.

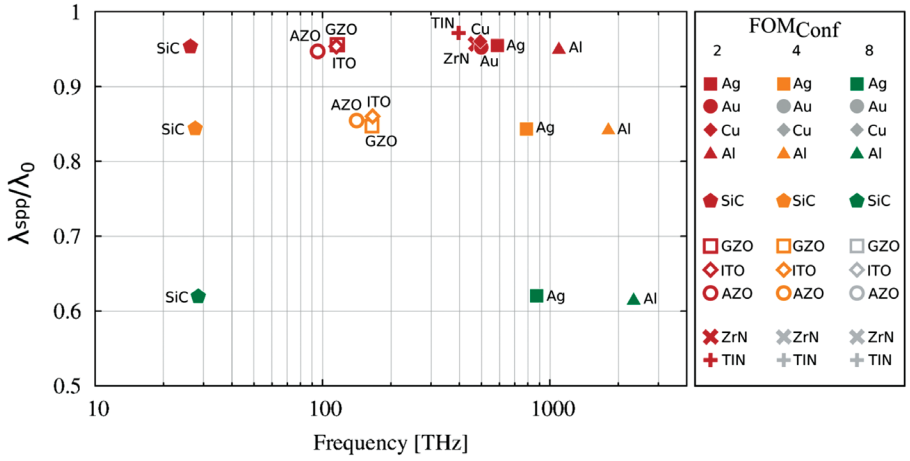

Figure 5 Ratio of the surface plasmon wavelength (λ_{spp}) over the free-space wavelength (λ_0) at three different FOM_{Conf}.

Acknowledgments: Work at Ames Laboratory was partially supported by the US Department of Energy, Office of Basic Energy Science, Division of Materials Science and Engineering (Ames Laboratory is operated for the US Department of Energy by Iowa State University under Contract No. DE-AC02-07CH11358), and by the US Office of Naval Research, Award No. N00014-14-1-0474. Work at FORTH was supported by the European Research Council under the ERC Advanced Grant No. 320081 (PHOTOMETA).

References

[1] Smith DR, Pendry JB, Wiltshire MCK. Metamaterials and negative refractive index. Science 2004;305:788–92.
[2] Soukoulis CM, Linden S, Wegener M. Negative refractive index at optical wavelengths. Science 2007;315:47–9.
[3] Liu Y, Zhang X. Metamaterials: a new frontier of science and technology. Chem Soc Rev 2011;40:2494–507.
[4] Soukoulis CM, Wegener M. Past achievements and future challenges in the development of three-dimensional photonic metamaterials. Nat Photonics 2011;5:523–30.
[5] Luo X, Qiu T, Lu W, Ni Z. Plasmons in graphene: recent progress and applications. Mat Sci Eng R 2013;74:351–76.
[6] Pendry JB. Negative refraction makes a perfect lens. Phys Rev Lett 2000;85:3966.
[7] Pendry JB, Schurig D, Smith DR. Controlling electromagnetic fields. Science 2006;312:1780–2.
[8] Leonhardt U. Optical conformal mapping. Science 2006;312:1777.
[9] Tassin P, Koschny T, Kafesaki M, Soukoulis CM. A comparison of graphene, superconductors and metals as conductors for metamaterials and plasmonics. Nat Photonics 2012;6:259–64.
[10] Berini P, De Leon I. Surface plasmon-polariton amplifiers and lasers. Nat Photonics 2011;6:16–24.
[11] Pendry JB, Holden AJ, Robbins DJ, Stewart WJ. Magnetism from conductors and enhanced nonlinear phenomena. IEEE Trans MIT 1999;47:2075–84.
[12] Smith DR, Padilla WJ, Vier DC, Nemat-Nasser SC, Schultz S. Composite medium with simultaneously negative permeability and permittivity. Phys Rev Lett 2000;84:4184.

[13] Dolling G, Enkrich C, Wegener M, Soukoulis CM, Linden S. Low-loss negative-index metamaterial at telecommunication wavelengths. Opt Lett 2006;31:1800–2.
[14] Dolling G, Wegener M, Soukoulis CM, Linden S. Negative-index metamaterial at 780 nm wavelength. Opt Lett 2007;32:53–5.
[15] Garcia-Meca C, Hurtado J, Martí J, Martínez A, Dickson W, Zayats AV. Low-loss multilayered metamaterial exhibiting a negative index of refraction at visible wavelengths. Phys Rev Lett 2011;106:067402.
[16] Hess O, Pendry JB, Maier SA, Oulton RF, Hamm JM, Tsakmakidis KL. Active nanoplasmonic metamaterials. Nat Mater 2012;11:573–84.
[17] Huang Z, Koschny T, Soukoulis CM. Theory of pump-probe experiments of metallic metamaterials coupled to a gain medium. Phys Rev Lett 2012;108:187402.
[18] Zhong XL, Li ZY. All-analytical semiclassical theory of spaser performance in a plasmonic nanocavity. Phys Rev B 2013;88:085101.
[19] Meinzer N, Ruther M, Linden S, Soukoulis CM, Khitrova G, Hendrickson J, Olitzky JD, Gibbs HM, Wegener M. Arrays of Ag split-ring resonators coupled to InGaAs single-quantum-well gain. Opt Express 2010;18:24140–51.
[20] Noginov MA, Zhu G, Belgrave AM, Bakker R, Shalaev VM, Narimanov EE, Stout S, Herz E, Suteewong T, Wiesner U. Demonstration of a spaser-based nanolaser. Nature 2009;460:1110–2.
[21] Kim J, Naik G, Emani N, Guler U, Boltasseva A. Modeling of seeded reflective modulators for DWDM systems. IEEE J Sel Top Quantum Electron 2013;19:4601907.
[22] Johnson PB, Christy RW. Optical constants of the noble metals. Phys Rev B 1972;6:4370.
[23] Ordal MA, Bell RJ, Alexander RW, Long LL, Querry MR. Optical properties of fourteen metals in the infrared and far infrared: Al, Co, Cu, Au, Fe, Pb, Mo, Ni, Pd, Pt, Ag, Ti, V, and W. Appl Opt 1985;24:4493–9.
[24] Naik GV, Shalaev VM, Boltasseva A. Alternative plasmonic materials: beyond gold and silver. Adv Mater 2013;25:3264–94.
[25] Naik GV, Kim J, Boltasseva A. Oxides and nitrides as alternative plasmonic materials in the optical range. Opt Mater Express 2011;1:1090–9.
[26] Economou EN. Surface plasmons in thin films. Phys Rev 1969;182:539.
[27] Jablan M, Buljan H, Soljačić M. Plasmonics in graphene at infrared frequencies. Phys Rev B 2009;80:245435.
[28] Fei Z, Rodin AS, Andreev GO, Bao W, McLeod AS, Wagner M, Zhang LM, Zhao Z, Thiemens M, Dominguez G, Fogler MM, Castro Neto AH, Lau CN, Keilmann F, Basov DN. Gate-tuning of graphene plasmons revealed by infrared nano-imaging. Nature 2012;487:82–5.
[29] Tassin P, Koschny T, Soukoulis CM. Graphene for terahertz applications. Science 2013;341:620–1.